JOURNAL OF GUIDANCE, CONTROL, AND DYNAMICS
Vol. 29, No. 1, January–February 2006

Spacecraft Formation Dynamics and Design

V. M. Guibout* and D. J. Scheeres†
University of Michigan, Ann Arbor, Michigan 48109

Previous research on the solutions of two-point boundary value problems is applied to spacecraft formation dynamics and design. The underlying idea is to model the motion of a spacecraft formation as a Hamiltonian dynamic system in the vicinity of a reference solution. Then the nonlinear phase flow can be analytically described using generating functions found by solving the Hamilton–Jacobi equation. Such an approach is very powerful and allows the study of any Hamiltonian dynamical systems independent of the complexity of its vector field and the solution of any two-point boundary value problem to be solved using only simple function evaluations. The details of the approach are presented through the study of a nontrivial example, the design of a formation in Earth orbit. For the analysis, the effect of the J_2 and J_3 gravity coefficients are taken into account. The reference trajectory is chosen to be an orbit with high inclination, $i = \pi/3$, and eccentricity, $e = 0.3$. Two missions are considered. First, given several tasks over a one-month period modeled as configurations at given times, the optimal sequence of reconfigurations to achieve these tasks with minimum fuel expenditure is found. Next, the theory is used to find stable configurations such that the spacecraft stay close to each other for an arbitrary but finite period of time. Both of these tasks are extremely difficult using conventional approaches, yet are simple to solve with the presented approach.

I. Introduction

SEVERAL missions and mission statements have identified formation flying as a means for reducing cost and adding flexibility to space-based programs. However, such missions raise a number of technical challenges because they require accurate dynamic models of the relative motion and control techniques to achieve formation reconfiguration and formation maintenance. There is a large body of literature on spacecraft formation flight that we will not attempt to survey in a systematic manner. On the one hand, we find articles that focus on analytical studies of the relative motion, and on the other hand, there is a large class of articles that develop numerical algorithms that solve specific reconfiguration and formation keeping problems. Theoretical studies require a dynamic model for the relative motion that is accurate and tractable. For that reason, the Clohessy–Wilshire (CW) equations, Hill's equations, or Gauss variational equations have often been used as a starting point. Using the CW equations, Hope and Trask[1] studied hover-type formation flying about the Earth, Vadali et al.[2] looked at periodic relative motion about the Earth, Gurfil and Kasdin[3] and Scheeres et al.[4] focused on formation keeping, Howell and Marchand[5] and Vadali et al.[6] analyzed relative motion in the vicinity of the libration points, and Vaddi et al.[7] studied the reconfiguration problem using impulsive thrusts. However, for a large class of orbits, these approximations do not hold: J_2 effects as well as a noncircular reference trajectory should be taken into account for low Earth orbits. As a result, past researchers have modified the CW equations to take the J_2 gravity coefficient into consideration. These improved equations have been widely used: Alfriend and Schaub[8] studied periodic relative motion and Lovell et al.[9] analyzed formation reconfiguration with impulsive thrusts. The nonimpulsive thrust problem is usually solved by using optimal control theory (although there are some exceptions, for instance, Hsiao and Scheeres[10] and Hussein et al.[11]), and if the dynamic model is tractable, then analytical solutions for the feedback control law may be found (Mishne[12]). These analytical approaches allow one to perform qualitative analysis and provide insight into the dynamics of the relative motion. However, they cannot be used for actual mission design (although there are some exceptions[13]). Indeed, they have inherent drawbacks: They neglect higher-order terms in the dynamics, and their domain of validity in phase space is very restricted and difficult to quantify. In addition, methods based on the state transition matrix tend to be valid only over short time spans. However, numerical algorithms have been developed to design spacecraft formations using the true dynamics. Koon et al.[14] use Routh reduction to reduce the dimensionality of the system and then develop an algorithm based on the use of the Poincaré map to find pseudoperiodic relative motion in the gravitational field of the Earth (including the J_2 gravity coefficient only), Xu and Fitz-Coy[15] and Avanzini et al.[16] study formation maintenance as a solution to an optimal control problem that they solve using a genetic algorithm and a multiobjective optimization algorithm, respectively. Even though these methods use the exact dynamics and, therefore, can be used to solve a specific reconfiguration or formation maintenance problem, they fail (except the method in Ref. 14) to provide insight into the dynamics. In addition, as noticed by Wang and Hadaegh,[17] formation reconfiguration design is a combinatorial problem. As a result, the algorithms mentioned are not appropriate for reconfiguration design because they require excessive computation (to reconfigure a formation of N spacecraft, there are $N!$ possibilities in general).

The method we describe in this paper directly tackles these issues and should be viewed as a semi-analytic approach, because it consists of a numerical algorithm whose output is a polynomial approximation of the dynamics. As a consequence, we are able to use a very accurate dynamic model and to obtain tractable expressions describing the relative motion. A fundamental difference with previous studies is that we describe the relative motion, that is, the phase space in the vicinity of a reference trajectory, as two-point boundary-value problems, whereas it is usually described as an initial-value problem. Such a description of the phase space is very natural and convenient. For instance, the reconfiguration problem and the search for periodic formations can be naturally formulated as two-point boundary-value problems. Note that our approach only applies to Hamiltonian systems; therefore, it cannot count for the drag in general. However, if the problem that needs to be solved is formulated as an optimal control problem, then any forces can be taken into account because the Pontryagin maximum principle

Presented as Paper 2004-4736 at the AIAA/AAS Astrodynamics Specialist Conference, Providence, RI, 16–19 August 2004; received 7 September 2004; revision received 29 January 2005; accepted for publication 2 February 2005. Copyright © 2005 by the American Institute of Aeronautics and Astronautics, Inc. All rights reserved. Copies of this paper may be made for personal or internal use, on condition that the copier pay the $10.00 per-copy fee to the Copyright Clearance Center, Inc., 222 Rosewood Drive, Danvers, MA 01923; include the code 0731-5090/06 $10.00 in correspondence with the CCC.

*Graduate Student Research Assistant and Ph.D. Candidate, Department of Aerospace Engineering; guibout@umich.edu.

†Associate Professor, Department of Aerospace Engineering; scheeres@umich.edu. Associate Fellow AIAA.

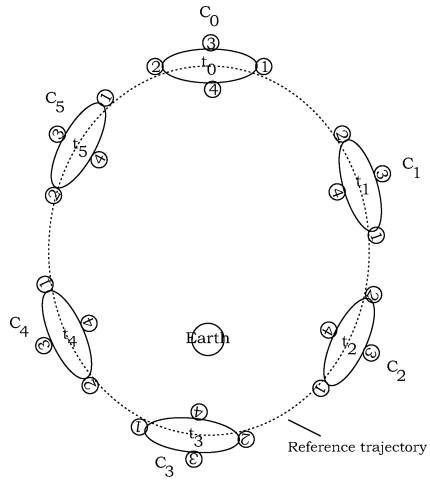

a) At each t_i, spacecraft must be in the configuration C_i

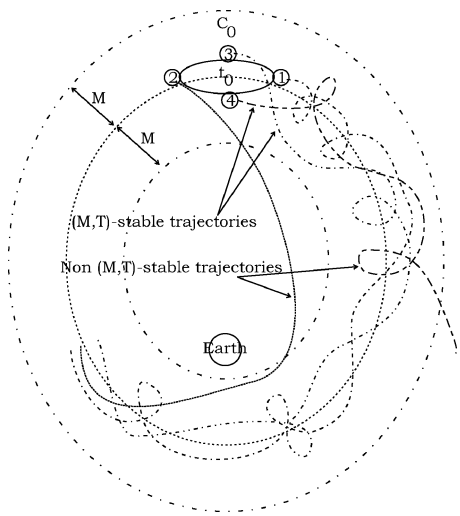

b) Stable and nonstable trajectories

Fig. 1 Two designs studied: multitask mission and search for stable configurations.

may yield a Hamiltonian two-point boundary-value problem (see Ref. 18), even if the dynamics are not Hamiltonian.

In the present paper, to showcase the strength of our method, we have chosen to study two challenging mission designs.

First, we consider a spacecraft formation about an oblate Earth (taking into account the J_2 and J_3 gravity coefficients) that must achieve five missions over a one month period. For each mission, the formation must be in a given configuration C_i that has been specified beforehand, and we wish to minimize the overall fuel expenditure. The configurations C_i are specified as relative positions of the spacecraft with respect to a specified reference trajectory (Fig. 1a). The C_i may be fully defined or have one degree of freedom. In our example, we require the spacecraft to be equally spaced on a circle centered on the reference trajectory at several epochs over the time period. The design of such a mission has several challenges.

1) The dynamics are nontrivial and nonintegrable.

2) The reference trajectory has high eccentricity and high inclination, and is not periodic.

3) Missions are planned a month in advance.

4) In our specific example, four spacecraft must achieve five missions. If one assumes that the C_i are fully defined, there are 7, 962, 624 ways of satisfying the missions.

5) The C_i may be defined by holonomic constraints and have an additional degree of freedom.

Second, we consider the design of stable formations. Given a reference trajectory, we wish to place the spacecraft in its vicinity and ensure that they remain close to each other over an extended period of time (Fig. 1b). This design is also very challenging.

1) The dynamics and the reference trajectory are nontrivial (as before).

2) Trajectories must not collide (except at the initial time for the deployment problem).

3) High accuracy in the initial conditions is required for long-term integration.

In the following sections, we first introduce the dynamic model as well as the reference trajectory. We then briefly recall the theory developed in Ref. 18 for the solution of these problems. Finally, we study the two missions discussed.

II. Problem Settings

The motion of a satellite under the influence of the Earth modeled by an oblate sphere (taking into account J_2 and J_3 gravity coefficients) in the fixed coordinate system (x, y, z) whose origin is the Earth center of mass is described by the following Hamiltonian:

$$\begin{aligned} H = {} & \tfrac{1}{2}\left(p_x^2 + p_y^2 + p_z^2\right) - 1\Big/\sqrt{x^2+y^2+z^2} \\ & \times \Big(1 - \left[R^2\Big/2r_0^2(x^2+y^2+z^2)\right]\{3[z^2/(x^2+y^2+z^2)] - 1\}J_2 \\ & - \left[R^3\Big/2r_0^3(x^2+y^2+z^2)^2\right]\{5[z^3/(x^2+y^2+z^2)] - 3z\}J_3\Big) \end{aligned} \tag{1}$$

where

$$GM = 398600.4405\ \mathrm{km^3 s^{-2}}, \qquad R = 6378.137\ \mathrm{km}$$

$$J_2 = 1.082626675 \times 10^{-3}, \qquad J_3 = 2.532436 \times 10^{-6} \tag{2}$$

All of the variables are normalized and r_0 is the radius of the trajectory at the initial time,

$$\begin{gathered} x \to x r_0, \qquad y \to y r_0, \qquad z \to z r_0 \\ t \to t\sqrt{r_0^3/GM}, \qquad p_x \to p_x\sqrt{GM/r_0} \\ p_y \to p_y\sqrt{GM/r_0}, \qquad p_z \to p_z\sqrt{GM/r_0} \end{gathered} \tag{3}$$

In the following paragraphs, we consider a reference trajectory the state of which is designated by (q^0, p^0) and study the relative motion of spacecraft with respect to it. The reference trajectory is chosen to be highly eccentric and inclined, but any other choice could have been considered. At the initial time, its state is

$$\begin{gathered} q_x^0 = r_p, \qquad q_y^0 = 0\ \mathrm{km}, \qquad q_z^0 = 0\ \mathrm{km}, \qquad p_x^0 = 0\ \mathrm{km \cdot s^{-1}} \\ p_y^0 = \sqrt{GM\Big/\tfrac{1}{2}(r_a + r_p)}\sqrt{r_a/r_p}\cos(\alpha)\ \mathrm{km \cdot s^{-1}} \\ p_z^0 = \sqrt{GM\Big/\tfrac{1}{2}(r_a + r_p)}\sqrt{r_a/r_p}\sin(\alpha)\ \mathrm{km \cdot s^{-1}} \\ \alpha = \pi/3\ \mathrm{rad}, \qquad r_p = 7000\ \mathrm{km}, \qquad r_a = 13{,}000\ \mathrm{km} \end{gathered} \tag{4}$$

Without the J_2 and J_3 gravity coefficients, the reference trajectory would be an elliptic orbit with eccentricity $e = 0.3$, inclination $i = \pi/3$ rad, argument of perigee $\omega = 0$, longitude of the ascending node $\Omega = 0$, semiminor axis $r_p = 7000$ km, semimajor axis $r_a = 13{,}000$ km, and of period $t_p = 2\pi\sqrt{\{(1/2^3)[(r_a + r_p)^3/r_p^3]\}}$ s ≈ 2 h 45 min. The Earth oblateness perturbation causes secular drifts in the eccentricity (due to J_3), in the argument of perigee (due to J_2 and J_3), and in the longitude of the ascending node (due to J_2 and J_3). (See Chobotov[19] for more details.) In addition, all of the orbit elements are subject to short- and long-period oscillations. In Figs. 2 and 3, the orbit elements for this trajectory are shown as a function of time during a day (about 10 revolutions about the Earth)

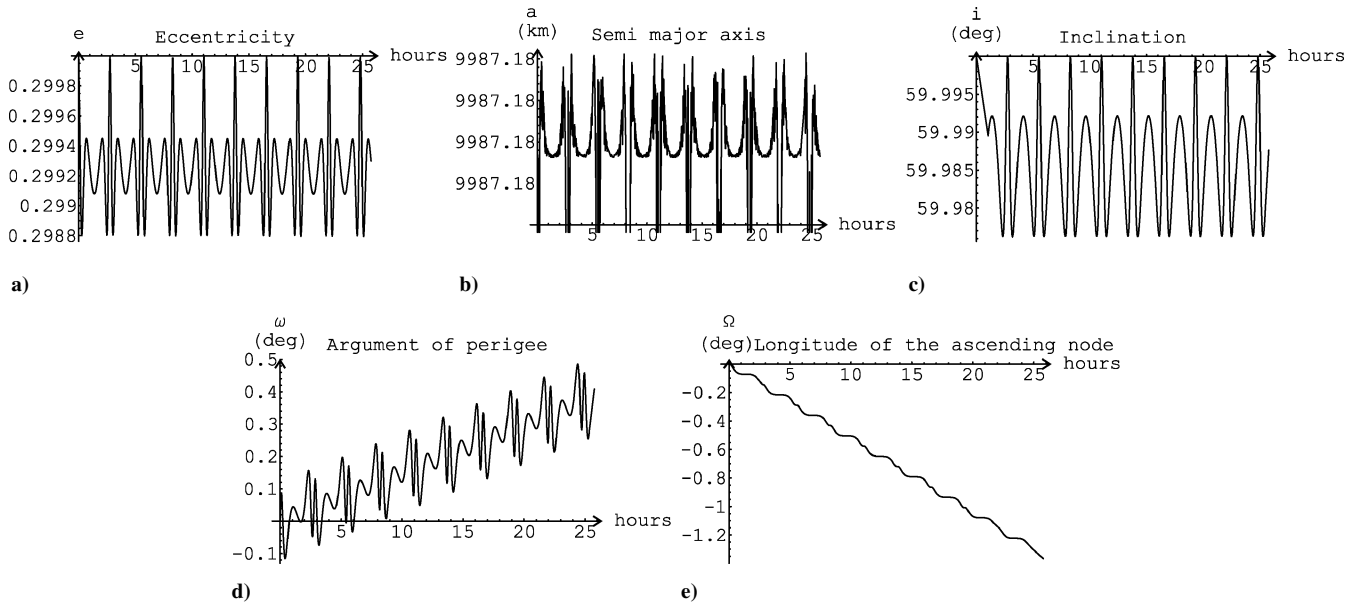

Fig. 2 Time history of orbital elements of reference trajectory during a day.

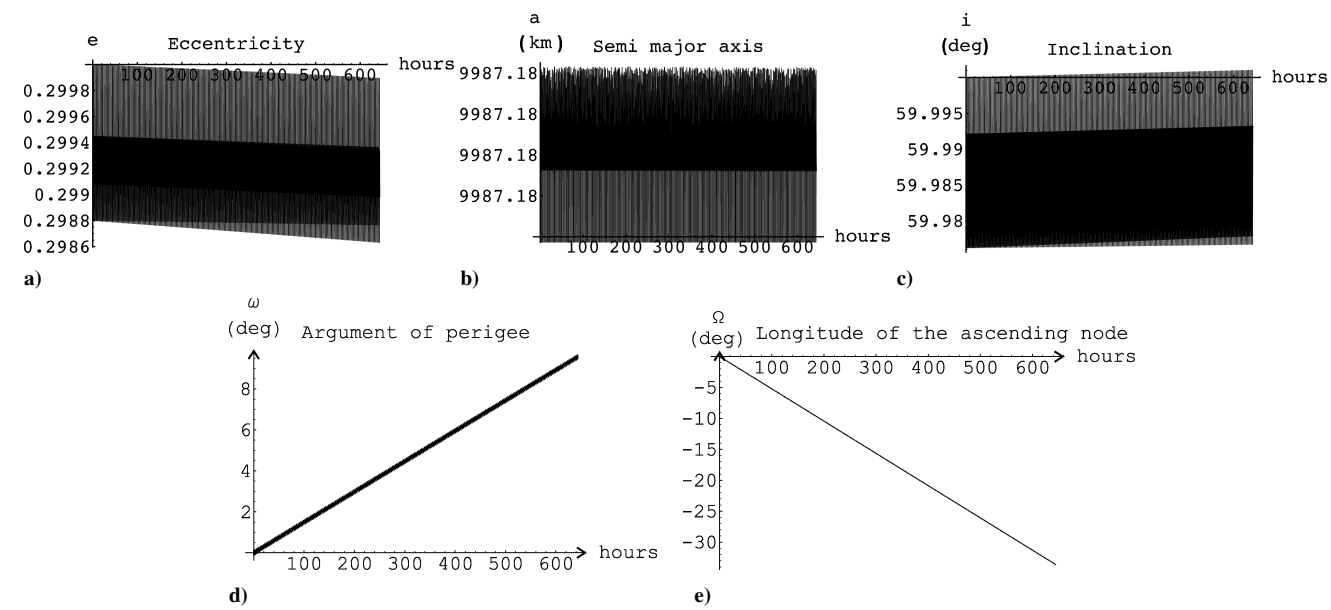

Fig. 3 Time history of orbital elements of reference trajectory over a month period.

and over a month period. The symplectic implicit Runge–Kutta integrator built in *Mathematica*© is used for integration of Hamilton's equations.

III. Algorithm

To study relative motion about the described reference trajectory, we use an algorithm whose output is an analytical description of the phase flow for the relative motion. It is based on previous studies by Guibout[18] and Guibout and Scheeres[20,22] on the Hamilton–Jacobi theory and essentially consists of solving the Hamilton–Jacobi partial differential equation for an approximation of the generating functions for the phase flow transformation describing the relative motion.

A. Relative Motion

The relative motion of a spacecraft the state of which is (q, p) moving in the Hamiltonian vector field defined by H [Eq. (1)] with respect to the reference trajectory $[q^0(t), p^0(t)]$ is described by the Hamiltonian function (see Ref. 20) H^h,

$$H^h(X^h, t) = \sum_{s=2}^{\infty} \sum_{\substack{i_1,\ldots,i_{2n}=0 \\ i_1+\cdots+i_{2n}=s}}^{s} \frac{1}{i_1!\cdots i_{2n}!} \times \frac{\partial^p H}{\partial q_1^{i_1}\cdots\partial q_n^{i_n}\partial p_1^{i_n+1}\cdots\partial p_n^{i_{2n}}}(q^0, p^0, t) X_1^{h^{i_1}}\cdots X_{2n}^{h^{i_{2n}}} \tag{5}$$

where $X^h = (\Delta q, \Delta p)$, $\Delta q = q - q^0$, and $\Delta p = p - p^0$ and where we assume X^h is small enough for the convergence of the series. Let us truncate the series in Eq. (5) to keep terms of order at most N. Then we say that the relative motion is described using an approximation of order N. Most past studies in the literature (CW, improved CW, and Hill's equations) consider an approximation of order two, that is, a linear approximation of the dynamics. (As mentioned in the Introduction, the improved CW equations are the CW equations that take into account the J_2 gravity coefficient.) Although such an

approximation is useful to obtain a first picture of the dynamical environment, as well as qualitative results, it cannot be used to design an actual formation for several reasons. First, nonlinear effects are usually not negligible, especially over a long time span. Second, linear effects may not be dominant over a short time span even though the Taylor series converges. Consider, for instance, the converging Taylor series of $(1-t)^x$ with respect to x. As t goes to 1, first terms are no longer dominant. (See Ref. 18 for a discussion on this issue.) The algorithm we have developed tackles these issues, N must be finite but can be as large as we want. There is no limit to the accuracy of the solution we obtain other than computer memory. (As we will see in the next section, if a solution up to order $N-1$ is known, we need to solve $[(N+5)!/N!5!]$ ordinary differential equations to obtain the Nth order.)

B. Solving Boundary Value Problems

The design of spacecraft formations can often be reduced to solving boundary-value problems. Indeed, the reconfiguration problem is a position-to-position boundary-value problem.[21] The search for periodic configurations, that is, spacecraft configurations that repeat themselves over time, may also be treated as a two-point boundary-value problem,[22] and we will see in this paper how one may find stable formations, that is, formations for which spacecraft naturally stay close to each other for a long time, as a solution to boundary-value problems. Finally, if a maneuver is set up as an optimal control problem, the necessary conditions for optimality can in many cases be reduced to a Hamiltonian system with known boundary values, that is, a two-point boundary-value problem (see Refs. 18 and 23).

Traditionally used to solve the equations of motion[24,25] analytically, the generating functions for the phase flow canonical transformation also allows one to solve two-point boundary-value problems.[18,20] Let us first consider a position q_0 to position q boundary-value problem and recall the generating function of the first kind $F_1(q, q_0, t)$,

$$p_i = \frac{\partial F_1}{\partial q_i}(q, q_0, t) \tag{6}$$

$$p_{0_i} = -\frac{\partial F_1}{\partial q_{0_i}}(q, q_0, t) \tag{7}$$

$$0 = H\left(q, \frac{\partial F_1}{\partial q}, t\right) + \frac{\partial F_1}{\partial t} \tag{8}$$

Equation (8) is known as the Hamilton–Jacobi equation and allows us to solve for the generating function F_1, whereas Eqs. (6) and (7) solve the boundary-value problem that consists in going from q_0 to q in t units of time.

Now let us consider more general generating functions. Let $(i_1, \ldots, i_p)(i_{p+1}, \ldots, i_n)$ and $(k_1, \ldots, k_r)(k_{r+1}, \ldots, k_n)$ be two partitions of the set $(1, \ldots, n)$ into two nonintersecting parts such that $i_1 < \cdots < i_p, i_{p+1} < \cdots < i_n, k_1 < \cdots < k_r$, and $k_{r+1} < \cdots < k_n$ and define $I_p = (i_1, \ldots, i_p)$, $\bar{I}_p = (i_{p+1}, \ldots, i_n)$, $K_r = (k_1, \ldots, k_r)$, and $\bar{K}_r = (k_{r+1}, \ldots, k_n)$. The generating function

$$F_{I_p,K_r}\left(q_{I_p}, p_{\bar{I}_p}, q_{0_{K_r}}, p_{0_{\bar{K}_r}}, t\right) = F\left(q_{i_1}, \ldots, q_{i_p}, p_{i_{p+1}}, \ldots, p_{i_n}, q_{0_{k_1}}, \ldots, q_{0_{k_r}}, p_{0_{k_{r+1}}}, \ldots, p_{0_{k_n}}, t\right) \tag{9}$$

verifies

$$p_{I_p} = \frac{\partial F_{I_p,K_r}}{\partial q_{I_p}}\left(q_{I_p}, p_{\bar{I}_p}, q_{0_{K_r}}, p_{0_{\bar{K}_r}}, t\right) \tag{10}$$

$$q_{\bar{I}_p} = -\frac{\partial F_{I_p,K_r}}{\partial q_{\bar{I}_p}}\left(q_{I_p}, p_{\bar{I}_p}, q_{0_{K_r}}, p_{0_{\bar{K}_r}}, t\right) \tag{11}$$

$$p_{0_{K_r}} = -\frac{\partial F_{I_p,K_r}}{\partial q_{0_{K_r}}}\left(q_{I_p}, p_{\bar{I}_p}, q_{0_{K_r}}, p_{0_{\bar{K}_r}}, t\right) \tag{12}$$

$$q_{0_{\bar{K}_r}} = \frac{\partial F_{I_p,K_r}}{\partial p_{0_{\bar{K}_r}}}\left(q_{I_p}, p_{\bar{I}_p}, q_{0_{K_r}}, p_{0_{\bar{K}_r}}, t\right) \tag{13}$$

$$0 = H\left(q_{I_p}, -\frac{\partial F_{I_p,K_r}}{\partial p_{\bar{I}_p}}, \frac{\partial F_{I_p,K_r}}{\partial q_{I_p}}, p_{\bar{I}_p}, t\right) + \frac{\partial F_{I_p,K_r}}{\partial t} \tag{14}$$

Equation (14) is the general form of the Hamilton–Jacobi equation and allows one to solve for the generating function F_{I_p,K_r}. On the other hand, Eqs. (10–13) solve the boundary-value problem that consists in going from $(q_{I_p}, p_{\bar{I}_p})$ to $(q_{0_{K_r}}, p_{0_{\bar{K}_r}})$ in t units of time. Among the 4^n generating functions defined earlier, we can recover the four classical kinds of generating functions discussed by Goldstein,[25] if the partitions are $(1, \ldots, n)()$ and $()(1, \ldots, n)$ (i.e., $p = n$ and $r = 0$) we recover the generating function F_2. The case $p = 0$ and $r = n$ corresponds to the generating function F_3, and if $p = 0$ and $r = 0$ we obtain F_4.

If the Hamiltonian in Eq. (14) is H^h, as defined by Eq. (5), then the generating functions are associated with the phase flow that describes the relative motion and they solve relative boundary-value problems. In terms of notation, (q_0, p_0, q, p) becomes $(\Delta q_0, \Delta p_0, \Delta q, \Delta p)$.

C. Numerics of the Algorithm

There are two methods for finding the generating functions: One can either solve the Hamilton–Jacobi equation [Eq. (14)] or use an indirect approach based on the initial-value problem. These methods are detailed in Ref. 18, and in the following paragraphs, we briefly review their characteristics. They both have their advantages and drawbacks, and one usually needs to combine both of them. We will discuss this issue at the end of this section.

1. *Solving the Hamilton–Jacobi Equation*

We assume the generating functions can be expressed as a Taylor series about the reference trajectory in its spatial variables,

$$F_{I_p,K_r}(y, t) = \sum_{s=2}^{\infty} \sum_{\substack{i_1, \ldots, i_{2n} = 0 \\ i_1 + \cdots + i_{2n} = s}}^{s} \frac{1}{i_1! \ldots i_{2n}!} f^{p,r}_{s,i_1,\ldots,i_{2n}}(t) y_1^{i_1} \ldots y_{2n}^{i_{2n}} \tag{15}$$

where $y = (\Delta q_{I_p}, \Delta p_{\bar{I}_p}, \Delta q_{0_{K_r}}, \Delta p_{0_{\bar{K}_r}})$. We substitute this expression into Eq. (14), where H is the Hamiltonian for the relative motion [(Eq. (5)]. The resulting equation is an ordinary differential equation that has the following structure:

$$P\left[y, f^{p,r}_{q,i_1,\ldots,i_{2n}}(t), \dot{f}^{p,r}_{i_1,\ldots,i_{2n}}(t)\right] = 0 \tag{16}$$

where P is a series in y with time-dependent coefficients that are functions of $f^{p,r}_{q,i_1,\ldots,i_{2n}}(t)$ and $\dot{f}^{p,r}_{q,i_1,\ldots,i_{2n}}(t)$. Equation (16) holds for all y if and only if all of the coefficients of P are zero. In this manner, we transform the ordinary differential equation (16) into a set of ordinary differential equations whose solutions are the coefficients of the generating function F_{I_p,K_r}. Now suppose that we have knowledge of the generating functions up to order $N-1$; then from Eq. (15), we deduce that we need to solve $(N+5)!/N!5!$ additional ordinary differential equations to find order N.

This approach provides us with a closed-form approximation of the generating functions. However, there are inherent difficulties because generating functions may develop singularities that prevent the integration from going further. (See Refs. 18, 26, and 27 for more details on singularities.) Techniques have been developed[18] to bypass this problem but have a cost in terms of computation. Typically, this method should only be used to solve generating functions over a short period of time.

2. *Indirect Approach*

By definition, generating functions implicitly define the canonical transformation they are associated with. Hence, we may compute the generating functions from the canonical transformation, that is, compute the generating functions for the phase flow transformation from knowledge of the phase flow. In this section, we develop an

algorithm based on these ideas. (More details may be gleaned in Ref. 18.)

Recall Hamilton's equations of motion for the relative motion,

$$\begin{pmatrix} \Delta\dot{q} \\ \Delta\dot{p} \end{pmatrix} = \begin{pmatrix} 0 & I_n \\ -I_n & 0 \end{pmatrix} \nabla H^h(\Delta q, \Delta p, t) \tag{17}$$

We suppose that $\Delta q(\Delta q_0, \Delta p_0, t)$ and $\Delta p(\Delta q_0, \Delta p_0, t)$ can be expressed as series in the initial conditions $(\Delta q_0, \Delta p_0)$ with time-dependent coefficients. We truncate the series to order N and insert these into Eq. (17). Hamilton's equations reduce to a series in $(\Delta q_0, \Delta p_0)$ whose coefficients depend on the time-dependent coefficients and the derivatives of the series $\Delta q(\Delta q_0, \Delta p_0, t)$ and $\Delta p(\Delta q_0, \Delta p_0, t)$. As in the preceding section, we balance terms of the same order and transform Hamilton's equations into a set of ordinary differential equations whose variables are the time-dependent coefficients defining Δq and Δp as a series in Δq_0 and Δp_0. Using $\Delta q(\Delta q_0, \Delta p_0, t_0) = \Delta q_0$ and $\Delta p(\Delta q_0, \Delta p_0, t_0) = \Delta p_0$ as initial conditions for the integration, we are able to compute an approximation of order N for the phase flow. At linear order, this approach recovers the state transition matrix. Then, a series inversion of the phase flow provides us with the gradient of the generating functions that can be integrated to find the generating functions.

The main advantage of this approach is that the phase flow is never singular; therefore, the system of ordinary differential equations is always well defined. However, this method requires us to solve more equations than the earlier method. If we want to find the generating function up to order N, then we need to solve six

$$\sum_{k=1}^{N-1} \frac{(k+5)!}{k!5!}$$

equations, which is always greater than

$$\sum_{k=2}^{N} \frac{(k+5)!}{k!5!}$$

the number of equations that need to be solved using the direct approach. The method provides us with the expression of the generating function at a given time only (the time at which we perform the series inversion). In addition, a symplectic algorithm should be used to integrate the ordinary differential equations; otherwise, we obtain an inconsistent expression of the gradient of the generating functions that cannot be integrated. (Some exactness conditions are not satisfied.[28])

In this paper, we combine both methods. We first solve the initial value problem over a long time span using the symplectic implicit Runge–Kutta integrator built in *Mathematica*. Then we compute the generating functions at a time of interest, for example, t_1, and solve the Hamilton–Jacobi equation about t_1, with initial conditions equal to the values of the generating functions at t_1 found using the indirect approach. For solving the Hamilton–Jacobi equation, we use the *Mathematica* built in function *ND Solve* with its default attributes. (*ND Solve* switches between a nonstiff Adams method and a stiff Gear method and achieves a precision of 10^{-10}.)

IV. Formation Design

In the preceding sections, we introduced a dynamic model, defined a reference trajectory, and presented an algorithm whose outputs are the generating functions associated with the phase flow describing the relative motion. We have also explained how these generating functions may be used to solve two-point boundary-value problems. We now combine all of these and use this combination to design spacecraft formations. We first use the combined algorithm to find the generating function F_1 up to order four, that is, we need to solve 498 ordinary differential equations in the indirect method, then proceed to a series inversion and solve the 203 ordinary differential equations given by the direct method. (See the Appendix for computational times.) After the generating functions are known, we can solve any position to position boundary-value problem with only six polynomial evaluations [Eqs. (6) and (7)].

A. Multitask Mission

We consider four imaging satellites flying in formation about the reference trajectory studied in the first part of this paper. We recall that it has high eccentricity, $e = 0.3$, high inclination, $i = \pi/3$, a semimajor axis of 13,000 km, and a semiminor axis of 7000 km. We want to plan spacecraft maneuvers over the next month knowing that they must observe the Earth, that is, must be in a given configuration C_i at the following instants (chosen arbitrarily for our study):

$$t_0 = 0, \qquad t_1 = 5 \text{ days } 22 \text{ h}, \qquad t_2 = 10 \text{ days } 20 \text{ h}$$
$$t_3 = 16 \text{ days } 2 \text{ h}, \qquad t_4 = 21 \text{ days } 14 \text{ h}, \qquad t_5 = 26 \text{ days } 20 \text{ h} \tag{18}$$

Define the local horizontal by the unit vectors $\hat{\boldsymbol{e}}_1, \hat{\boldsymbol{e}}_2$ such that $\hat{\boldsymbol{e}}_2$ is along $r^0 \times v^0$ and $\hat{\boldsymbol{e}}_1$ is along $\hat{\boldsymbol{e}}_2 \times r^0$. At every t_i, the configuration C_i is defined by the four following relative positions (or slots):

$$q^1 = 700 \text{ m}\,\hat{\boldsymbol{e}}_1, \qquad q^2 = -700 \text{ m}\,\hat{\boldsymbol{e}}_1$$
$$q^3 = 700 \text{ m}\,\hat{\boldsymbol{e}}_2, \qquad q^4 = -700 \text{ m}\,\hat{\boldsymbol{e}}_2 \tag{19}$$

Note that all of the q^i are in the local horizontal plane. In addition, at each t_i, q^1 is always in front of the reference state (in the local horizontal plane), q^2 is behind, q^3 is on the left, and q^4 is on the right (Fig. 1a). At each t_i, there must be one spacecraft per slot, and we want to determine the sequence of reconfigurations that minimizes the total fuel expenditure. Each impulse instantaneously changes the velocity vector. The norm of these changes quantifies the fuel expenditure. (Other cost functions such as equal fuel consumption for each spacecraft may be considered as well.) For the first mission, there are 4! configurations (number of permutation of the set $\{1, 2, 3, 4\}$). For the second mission, for each of the previous 4! configurations, there are again 4! configurations, that is, a total of $4!^2$ possibilities. Thus, for five missions there are $4!^5 = 7,962,624$ possible configurations.

In this paper, we focus on impulsive controls, but the method we develop can equivalently apply to continuous thrust problems. Indeed, continuous thrust problems are usually solved using optimal control theory and reduce to a set of necessary conditions that are formulated as a Hamiltonian two-point boundary-value problem. This boundary-value problem can in turn be solved using the method we present in this paper.[23] Let us now design the described mission. We assume impulsive controls that consist of impulsive thrusts applied at $t_{i \in [0,5]}$. For each of the four spacecraft, we need to compute the velocity at t_i so that the spacecraft moves to its position specified at t_{i+1} under gravitational forces only. As a result, we must solve $5 \cdot 4! = 120$ position-to-position boundary-value problems. (Given two positions at t_i and t_{i+1}, we need to compute the associated velocity.) When the generating functions are used, this problem can be handled at the cost of only 120 function evaluations. (Computation times are given in the Appendix.) Then, we need to evaluate the fuel expenditure (sum of the norm of all of the required impulses, assuming zero relative velocities at the initial and final times) for all of the permutations to find the sequence that minimizes the cost function. (There are 7, 962, 624 combinations.) In Fig. 4, the number of configurations as a function of the values of the cost function are shown. Notice that most of the configurations require at least three times more fuel than the best configuration and less than 6% yield values of the cost function that are less than twice the value associated with the best configuration. The cost function for the optimal sequence of reconfigurations is $0.00644 \text{ km} \cdot \text{s}^{-1}$, whereas it is $0.0396 \text{ km} \cdot \text{s}^{-1}$ in the least optimal design. In the optimal case, the four spacecraft have the following positions.

Spacecraft 1 has (t_0, q^1), (t_1, q^2), (t_2, q^2), (t_3, q^2), (t_4, q^2), (t_5, q^2).

Spacecraft 2 has (t_0, q^2), (t_1, q^1), (t_2, q^1), (t_3, q^1), (t_4, q^1), (t_5, q^1).

Spacecraft 3 has (t_0, q^3), (t_1, q^4), (t_2, q^4), (t_3, q^4), (t_4, q^3), (t_5, q^4).

Spacecraft 4 has (t_0, q^4), (t_1, q^3), (t_2, q^3) (t_3, q^3), (t_4, q^4), (t_5, q^3).

Whereas the worst scenario corresponds to the following positions.

Spacecraft 1 has (t_0, q^1), (t_1, q^1), (t_2, q^2), (t_3, q^2), (t_4, q^1), (t_5, q^2).

Spacecraft 2 has (t_0, q^2), (t_1, q^2), (t_2, q^3), (t_3, q^4), (t_4, q^4), (t_5, q^3).

Spacecraft 3 has $(t_0, q^3), (t_1, q^3), (t_2, q^1)\ (t_3, q^3), (t_4, q^3), (t_5, q^4)$.

Spacecraft 4 has $(t_0, q^4), (t_1, q^4), (t_2, q^4)\ (t_3, q^1), (t_4, q^2), (t_5, q^1)$.

We may verify, a posteriori, whether the solutions found meet the mission goals, that is, if the order four approximation of the dynamics is sufficient to simulate the true dynamics. Explicitly comparing the analytical solution with numerically integrated results shows that the spacecraft are at the desired positions at every t_i with a maximum error of 1.5×10^{-8} km. As a comparison, an order two approximation of the dynamics would yield a maximum error of 0.116865 km. Such an error is not acceptable for a realistic design and justifies the need for higher-order solutions.

Our algorithm does not consider the risk of collision in the design. However, it provides a simple way to check afterward if there is collision. Recall the indirect method; it is based on the initial-value problem and essentially consists in solving Hamilton's equations for an approximation of the flow. Once such a solution is found, we can generate any trajectory at the cost of a function evaluation, there is no need to integrate Hamilton's equations again. Checking for collisions is again a combinatorial problem, and therefore, our approach is particularly adapted to this. As an example, let us verify if the design we proposed for the multitask mission yields collisions.

It can be proven that for this specific mission, there is no design that prevents the relative motion of the spacecraft to be less than 100 m. (Fig. 5 shows the relative distances for optimal design.) In the best scenario, the smallest relative distance between the spacecraft is about 15 m and is achieved in 3360 different designs. Among these 3360 possibilities, we show in Fig. 6 the time history of the relative distance between the spacecraft for the design that achieves minimum fuel expenditure. (The total fuel expenditure is 60% larger than in the best case.) This scenario corresponds to the spacecraft having the following positions.

Spacecraft 1 has (t_0, q^1), (t_1, q^2), (t_2, q^3), (t_3, q^3), (t_4, q^4), (t_5, q^3).

Spacecraft 2 has (t_0, q^2), (t_1, q^3), (t_2, q^4), (t_3, q^4), (t_4, q^3), (t_5, q^4).

Spacecraft 3 has $(t_0, q^3), (t_1, q^4), (t_2, q^1)\ (t_3, q^2), (t_4, q^1), (t_5, q^2)$.

Spacecraft 4 has $(t_0, q^4), (t_1, q^1), (t_2, q^2)\ (t_3, q^1), (t_4, q^2), (t_5, q^1)$.

For times at which the spacecraft are close to each other, we may use some local control laws to perform small maneuvers for ensuring appropriate separation.

Another option consists of changing the configurations at t_i so that there exists a sequence of reconfigurations such that the relative distance between the spacecraft stays larger than 100 m. This can easily be done using our approach because F_1 is already known. Solving a new design would only require 120 evaluations of the gradient of F_1.

In the preceding example, we take advantage of our algorithm to perform the required design, that is, we are able to plan missions involving several spacecraft over a month using nontrivial dynamics while minimizing a given cost function. Such a design is possible because we focus directly on specifying the problem as a series of boundary-value problems. Solution of this problem using a more traditional approach for solving boundary-value problems would have required direct integration of the equations of motion for each of the 120 boundary-value problems.

However, we have not taken full advantage of our algorithm yet because this example does not provide insight on the dynamics. We now consider a different mission to remedy this and show how our algorithm may be used for analytical studies.

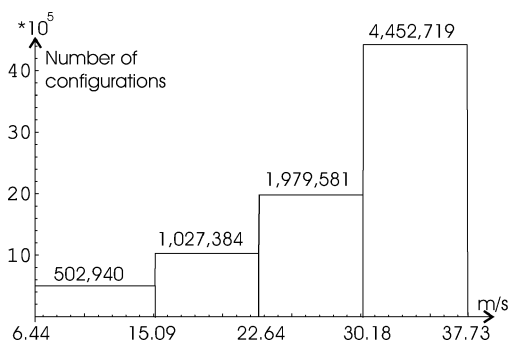

Fig. 4 Number of configurations as function of value of cost function.

B. Different Multitask Mission

For simplicity, we assume that the spacecraft must achieve only one task, that is, we constrain the geometry of the formation at t_0 and t_1. However, instead of imposing absolute relative positions, we only require the spacecraft to be equally spaced on a circle of a given radius in the local horizontal plane at t_1. Such a constraint is more realistic, especially for imaging satellites because rotations

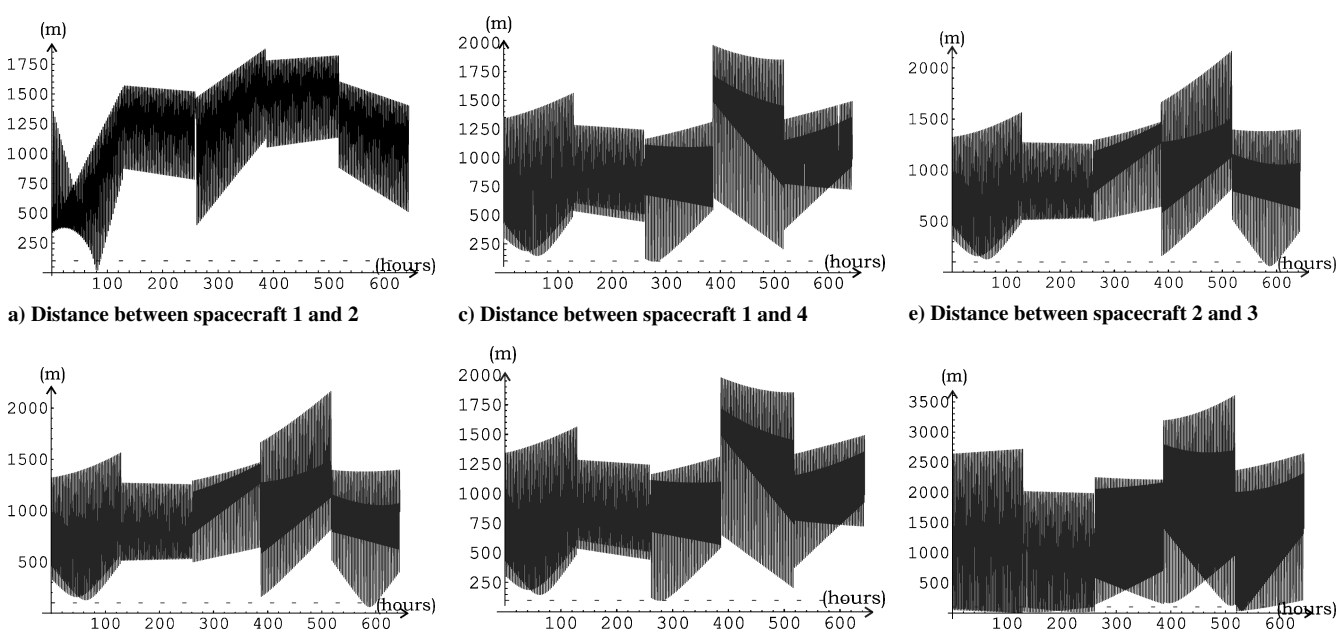

a) Distance between spacecraft 1 and 2

c) Distance between spacecraft 1 and 4

e) Distance between spacecraft 2 and 3

b) Distance between spacecraft 1 and 3

d) Distance between spacecraft 2 and 3

f) Distance between spacecraft 3 and 4

Fig. 5 Distance between spacecraft as function of time.

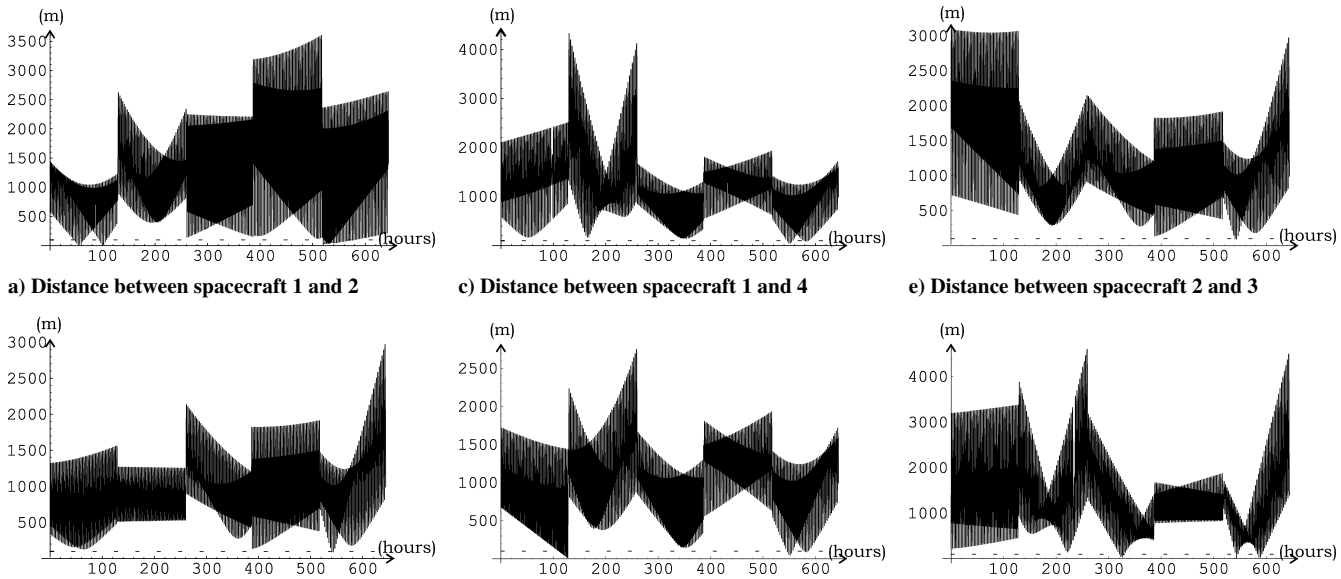

a) Distance between spacecraft 1 and 2

c) Distance between spacecraft 1 and 4

e) Distance between spacecraft 2 and 3

b) Distance between spacecraft 1 and 3

d) Distance between spacecraft 2 and 3

f) Distance between spacecraft 3 and 4

Fig. 6 Distance between spacecraft as function of time.

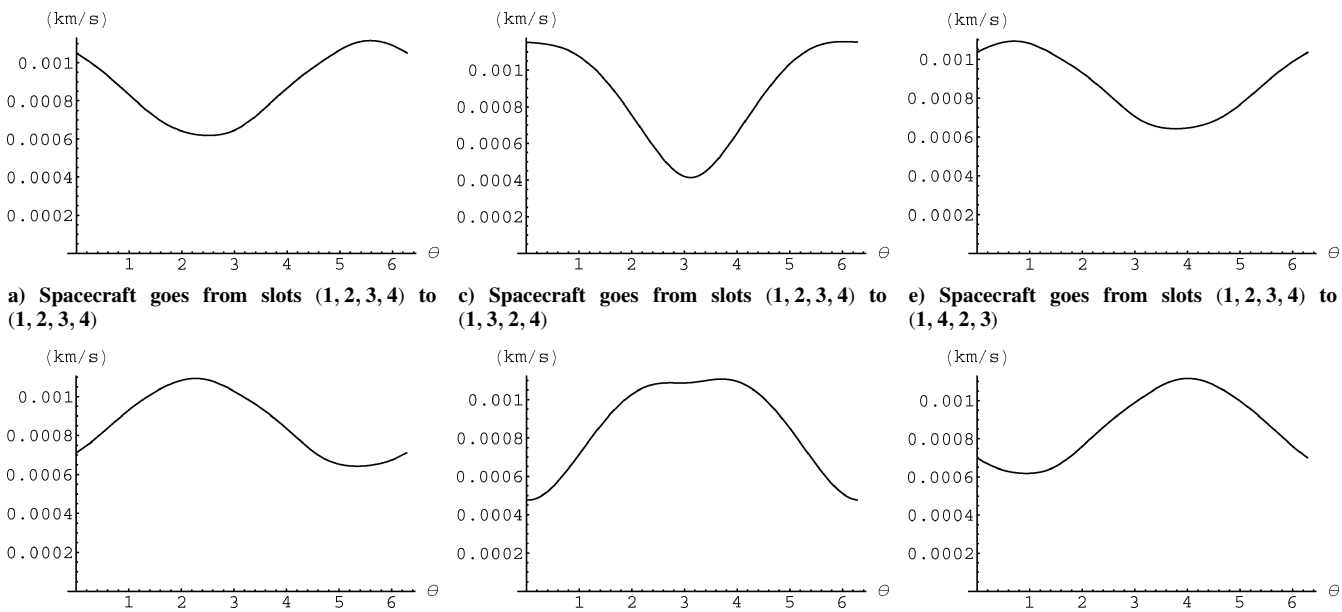

a) Spacecraft goes from slots (1, 2, 3, 4) to (1, 2, 3, 4)

c) Spacecraft goes from slots (1, 2, 3, 4) to (1, 3, 2, 4)

e) Spacecraft goes from slots (1, 2, 3, 4) to (1, 4, 2, 3)

b) Spacecraft goes from slots (1, 2, 3, 4) to (1, 2, 4, 3)

d) Spacecraft goes from slots (1, 2, 3, 4) to (1, 3, 4, 2)

f) Spacecraft goes from slots (1, 2, 3, 4) to (1, 4, 3, 2)

Fig. 7 Cost function as function of θ for each configuration.

of the formation about the local vertical should not influence performance. In this problem, combinatorics and smooth functional analysis are mixed together. Indeed, the positions of the four slots are given by a variable θ. (Here, θ indicates the position of the first slot; the other slots are determined from the constraint that they should be equally spaced.) Then, we need to solve a combinatorial problem as in the preceding case. To find the θ that minimizes the cost function, we use the polynomial approximation of the generating functions provided by our algorithm to express the cost function as a one-dimensional polynomial in θ. Variations of the cost function are determined analytically by computing the derivative of the cost function.

We choose the initial position to be as in the earlier example and require the spacecraft to be equally spaced at t_1 on a circle of radius 700 m in the local horizontal plane. In addition, we assume zero relative velocities at the initial and final times and again choose the cost function to be the sum of the norm of the required impulses. As before, $\hat{\boldsymbol{e}}_1, \hat{\boldsymbol{e}}_2$ span the local horizontal plane, and we define θ as the angle between the relative position vector and $\hat{\boldsymbol{e}}_1$. Because θ is allowed to vary from 0 to 2π, that is, slot 1 describes the whole circle as θ goes from 0 to 2π, we may consider that spacecraft 1 always goes from slot 1 to slot 1. As a consequence, there are 3! free configurations. In Fig. 7, we show the values of the cost function as a function of θ for each of the configurations. The best design is the one for which $\theta = 3.118$ rad, spacecraft 1 goes from slot 1 to slot 1, spacecraft 2 from slot 2 to slot 3, spacecraft 3 from slot 3 to slot 2 and spacecraft 4 from slot 4 to slot 4 (Fig. 7c).

If several missions need to be planned, then a new variable is introduced for each and a multivariable polynomial must be studied. As a result, minima of the cost function are found by evaluating as many derivatives as there are missions.

Through this example, we have gained insight on the dynamics by using the analytical approximation of the generating function and were able to solve the fuel optimal reconfiguration problem.

The method we use is very general and can be applied to solve any reconfiguration problem given that the constraints on the configurations are holonomic.

C. Stable Trajectories

Now we focus on another crucial, but difficult, design issue for spacecraft formations. We search for configurations, called stable configurations, such that the spacecraft stay close to the reference trajectory over a long time span.

1. Definitions

Let us first define the notion of stable formation more precisely. Let T be a given instant and M a positive real number.

Definition 1 (stable relative trajectory): A relative trajectory between two spacecraft is (M, T) stable if and only if their relative distance never exceeds M over the time span $[0, T]$.

Definition 2 (stable formation): A formation of spacecraft is (M, T) stable if and only if all of the spacecraft have (M, T) stable relative trajectories with respect to the reference trajectory.

Periodic formations are instances of stable formations; they are (M, ∞) stable. Also note that our definition recovers the notion of Lyapunov and Lagrange stability: Lyapunov stable relative trajectories are (M, ∞) stable and (M, T) stable trajectories are Lagrange stable for a finite period T. In this paper, we focus on (M, T) stable formations with T large but finite; the approach we present is not appropriate to find (M, ∞) stable configurations. However, when the reference trajectory is periodic, Guibout and Scheeres[22] developed a technique based on generating functions and Hamilton–Jacobi theory to find periodic configurations.

2. Stable Trajectories as Solutions to Two-Point Boundary-Value Problems

To use the theory we have presented above, we formulate the search for stable trajectories as two-point boundary-value problems.

Define the local vertical plane as the two-dimensional vector space perpendicular to the velocity vector of the reference trajectory. In other words, the local vertical is spanned by $\hat{\boldsymbol{f}}_1, \hat{\boldsymbol{f}}_2$, where $\hat{\boldsymbol{f}}_1$ and $\hat{\boldsymbol{f}}_2$ are two unit vectors along $\boldsymbol{r}^0 \times \boldsymbol{v}^0$ and $\boldsymbol{v}^0 \times \hat{\boldsymbol{f}}_1$, respectively. In the local vertical plane, we use polar coordinates, $(r - r^0, \theta)$ where θ is the angle between $\hat{\boldsymbol{f}}_1$ and the local relative position vector $\boldsymbol{r} - \boldsymbol{r}^0$. We denote by $\mathcal{C}_t^r$ the circle of radius r centered on the reference trajectory that lies in the local vertical plane at t. A position on this circle is fully determined by θ (Fig. 8). Then given instant $t_f > t_0$ and a distance $r_f > 0$, the circle $\mathcal{C}_{t_f}^{r_f}$ is defined.

Before searching for stable configurations, we first introduce a new methodology to find (M, T) stable relative trajectories for a single spacecraft about the defined reference trajectory. Consider the following two-point boundary-value problem. Find all trajectories going from the initial position of the spacecraft to any point on $\mathcal{C}_{t_f}^{r_f}$ in $t_f - t_0$ units of time where $r_f < M$ (Fig. 9).

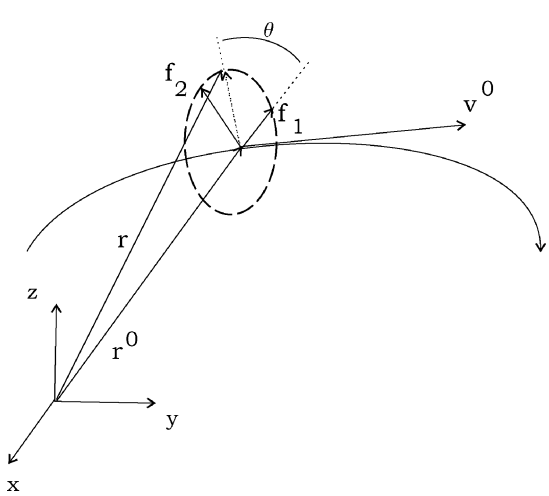

Fig. 8 Local geometry.

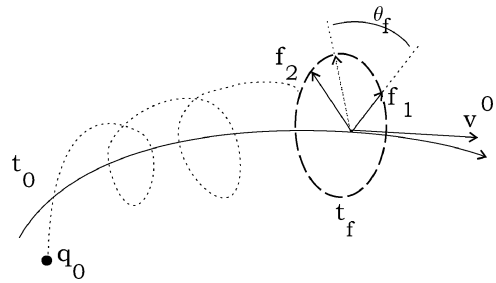

Fig. 9 Boundary-value problem.

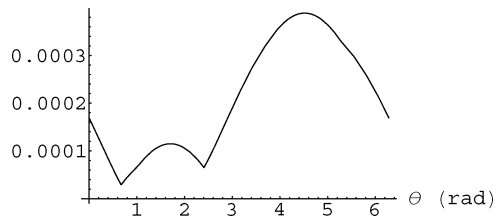

Fig. 10 Cost function as function of θ_f at $t - 259$ h, 13 min.

Solutions to this boundary-value problem have the following properties.

1) They contain (M, T) stable relative trajectories.

2) They contain relative trajectories that are not (M, T) stable, that is, trajectories that go far from the reference trajectory in the time interval $(0, t_f)$ but come back close to the reference trajectory at t_f. We point out that many of these trajectories are ignored by our algorithm because it uses a local approximation of the dynamics.

On the other hand, we know that stable trajectories must have similar orbit elements, as compared to the reference trajectory. Therefore, to discriminate between the solutions to the two-point boundary-value problem, we can use orbit elements especially because we know, a priori, that the longitude of the ascending node and the argument of perigee have secular drifts. This leads us to define a cost function J as

$$J = \tfrac{1}{4}\left\|\Delta\omega_{t_f}\right\| + \tfrac{1}{4}\left\|\Delta\omega_{t_f} - \Delta\omega_{t_0}\right\| + \tfrac{1}{4}\left\|\Delta\Omega_{t_f}\right\| + \tfrac{1}{4}\left\|\Delta\Omega_{t_f} - \Delta\Omega_{t_0}\right\| \tag{20}$$

where $\|\Delta\omega_{t_f}\|$ corresponds to the relative argument of perigee at t_f, that is, the difference at t_f between the argument of perigee of the spacecraft trajectory and the argument of perigee of the reference trajectory, $\|\Delta\omega_{t_f} - \Delta\omega_{t_0}\|$ characterizes the change in the relative argument of perigee between t_0 and t_f and the other terms are similar and involve the longitude of the ascending node instead.

Let us now consider the following boundary-value problem. Find all trajectories going from the initial position of the spacecraft to any point on $\mathcal{C}_{t_f}^{r_f}$ in $t_f - t_0$ units of time that minimize J.

From the discussion, we conclude that solutions to this boundary-value problem characterize stable relative trajectories. Using this criterion, we do not have an accurate control over M. If (M, T) stable trajectories are searched, then r_0 and r_f must be chosen to be less than M. However, we have no guarantee that the relative distance is less than M for all $t \le T$. By minimizing J, we find (M', T') stable trajectories where M' is close to M but may be superior. (See the subsequent example.) In addition, because the trajectories found have similar orbit elements (due to the terms $\|\Delta\omega_{t_f}\|$ and $\|\Delta\Omega_{t_f}\|$ in the cost function), T' is generally larger than $t_f = T$.

3. Methodology

We showed earlier that the search for stable trajectories reduces to solving a two-point boundary-value problem while minimizing a given cost function. In this section, we solve this problem using the generating function theory introduced in the first part of this paper.

First, we notice that F_1 solves the boundary-value problem that consists of going from an initial position q_0 to a position q_f in t_f

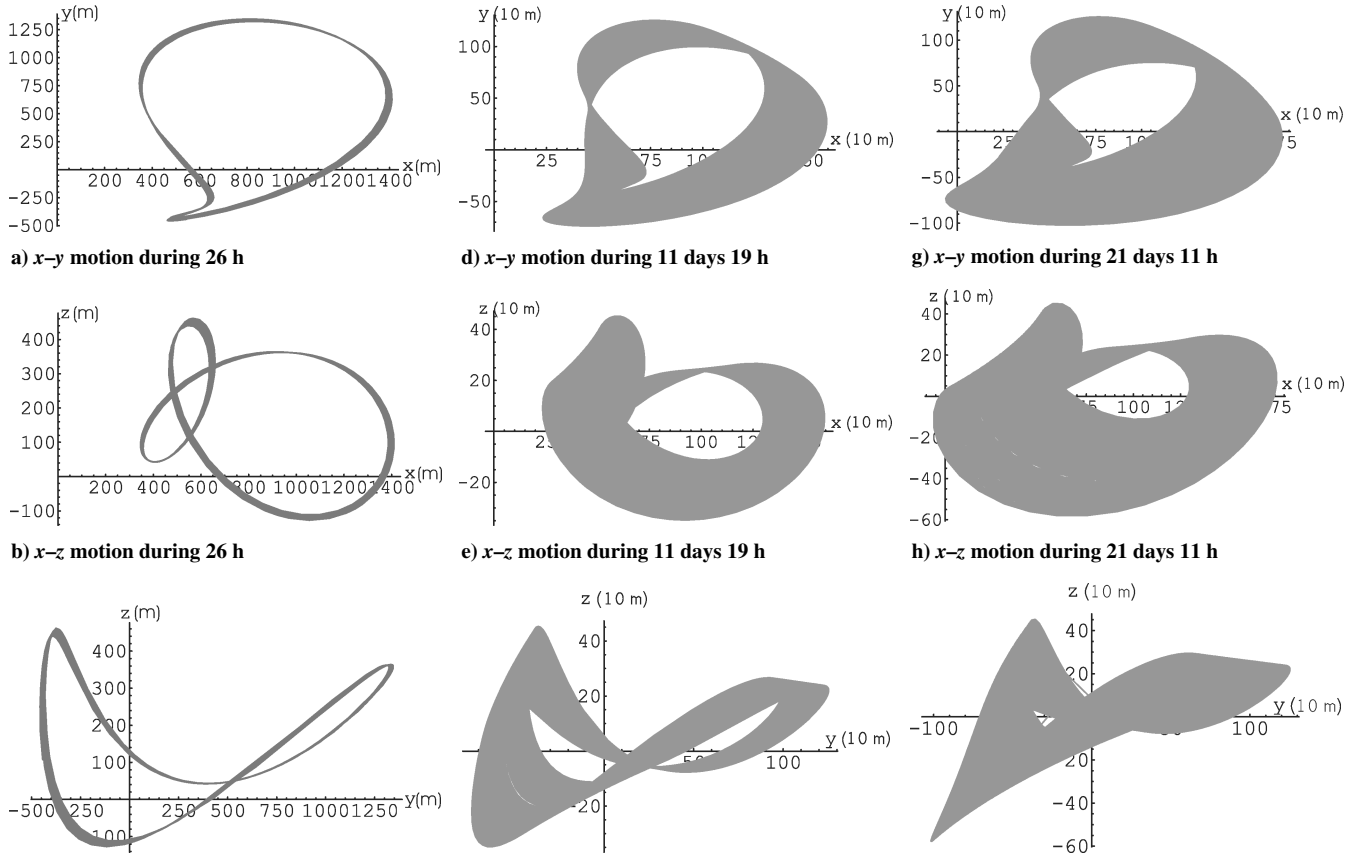

a) *x–y* motion during 26 h

b) *x–z* motion during 26 h

c) *y–z* motion during 26 h

d) *x–y* motion during 11 days 19 h

e) *x–z* motion during 11 days 19 h

f) *y–z* motion during 11 days 19 h

g) *x–y* motion during 21 days 11 h

h) *x–z* motion during 21 days 11 h

i) *y–z* motion during 21 days 11 h

Fig. 11 Trajectory associated with minimum $\theta_f = 0.671503$ rad, $t_f = 10$ days, 19 h, 13 min.

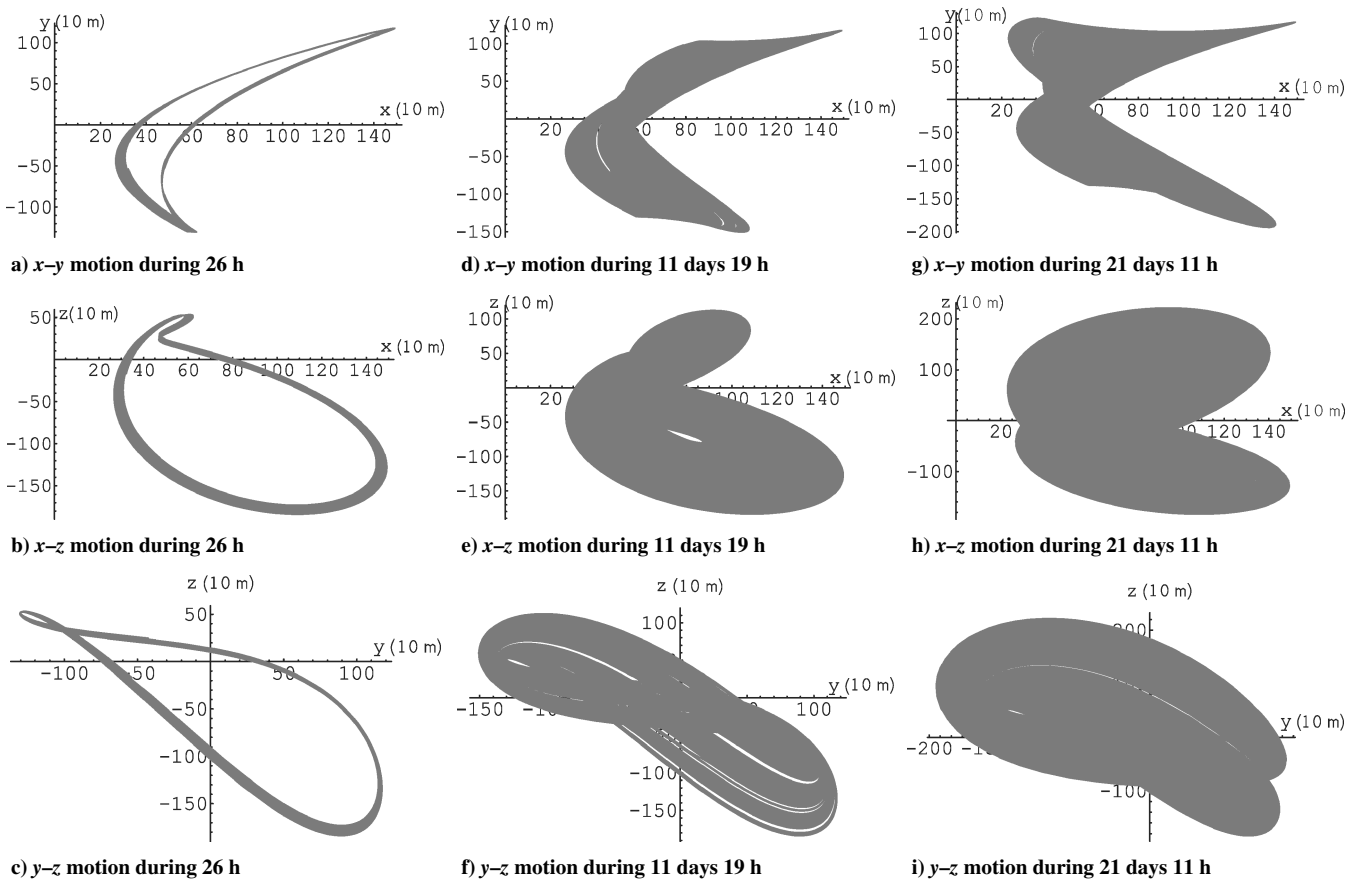

a) *x–y* motion during 26 h

b) *x–z* motion during 26 h

c) *y–z* motion during 26 h

d) *x–y* motion during 11 days 19 h

e) *x–z* motion during 11 days 19 h

f) *y–z* motion during 11 days 19 h

g) *x–y* motion during 21 days 11 h

h) *x–z* motion during 21 days 11 h

i) *y–z* motion during 21 days 11 h

Fig. 12 Trajectory associated with the minimum $\theta_f = 2.4006615$ rad, $t_f = 10$ days, 19 h, 13 min.

units of time. Indeed, from Eqs. (6) and (7) we have

$$p_0 = -\frac{\partial F_1}{\partial q_0}(q_f, q_0, t_f) \tag{21}$$

$$p_f = \frac{\partial F_1}{\partial q}(q_f, q_0, t_f) \tag{22}$$

Then we assume that q_f describes $\mathcal{C}_{t_f}^{r_f}$, that is, $q_f = r_f \cos(\theta_f)\hat{\boldsymbol{f}}_1 + r_f \sin(\theta_f)\hat{\boldsymbol{f}}_2$, where θ_f ranges from 0 to 2π. Because F_1 is approximated by a polynomial in (q_f, q_0) with time-dependent coefficients, Eqs. (21) and (22) allow us to express p_0 and p_f as polynomials in θ_f with time-dependent coefficients. Finally, with knowledge of $p_0(\theta_f)$, $p_f(\theta_f)$, q_0, and $q_f(\theta_f)$, we can express J as a function of θ_f and easily find its minima $\{\theta_f^1, \ldots, \theta_f^r\}$. Stable trajectories are then those that travel from q_0 to $q_f = r_f \cos(\theta_f^i)\hat{\boldsymbol{f}}_1 + r_f \sin(\theta_f^i)\hat{\boldsymbol{f}}_2$, $i \in [1, r]$ in t_f units of time.

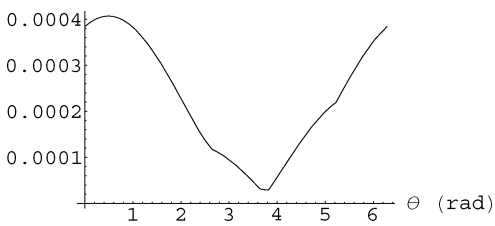

Fig. 13 Cost function as function of θ_f at $t = 258$ h, 19 min.

4. Example

Let us illustrate this procedure by searching for stable trajectories for a spacecraft whose initial position relative to the reference trajectory is $q_0 = (495, -428.6, 247.5)$ m in the inertial frame or equivalently $q_0 = 700\cos(\pi/4)\hat{\boldsymbol{f}}_1 + 700\sin(\pi/4)\hat{\boldsymbol{f}}_2$ m. Again the reference trajectory considered here was presented in the Introduction. It has high eccentricity and high inclination. We use the generating function computed in earlier examples, that is, an order four approximation of the dynamics. In addition, $t_f = 10$ days, 19 h, 13 min and $r_f = 700$ m. Then, using a symbolic manipulator, we express J as a function of θ_f and show its values in Fig. 10. It has two local minima at $\theta_1 = 0.671503$ and $\theta_2 = 2.4006615$ rad that correspond to stable trajectories. The relative motions associated with these two trajectories are in Figs. 11 and 12, shown over time spans smaller and larger than t_f. We note the excellent behavior of these trajectories: They remain stable over a time interval larger than the one initially considered. Also notes that one of the trajectories (Fig. 11) is (r_f, t_f) stable, whereas the other one (Fig. 12) is $(3r_f, t_f)$ stable.

Before going further, let us discuss the role played by t_f. We transformed the search for stable trajectories into a boundary-value problem over a time span defined by t_f that we apparently chose arbitrarily. By varying t_f, we notice that minima of the cost function correspond to different stable trajectories. In Fig. 13 we show the cost function as a function of θ_f for $t = t_f - 1$ h, 6 min $= 10$ days 18 h 19 min. In contrast to the earlier case, the cost function has only one minimum at $\theta = 3.814575$ rad. In Fig. 14 we present the trajectory that corresponds to this minimum. It is stable but different from the preceding ones (Figs. 11 and 12). This result was expected and makes our approach even more valuable. Indeed, because we

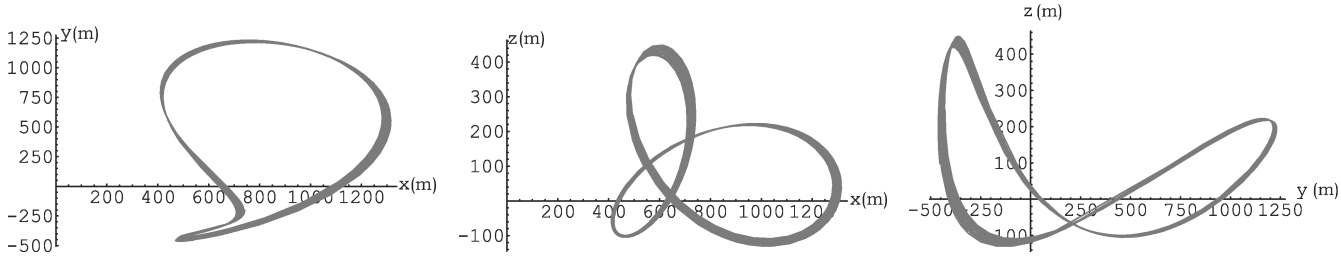

a) x–y motion during 26 h **b) x–z motion during 26 h** **c) y–z motion during 26 h**

Fig. 14 Trajectory associated with the minimum $\theta_f = 3.814575$ rad, $t_f = 10$ days, 18 h, 19 min.

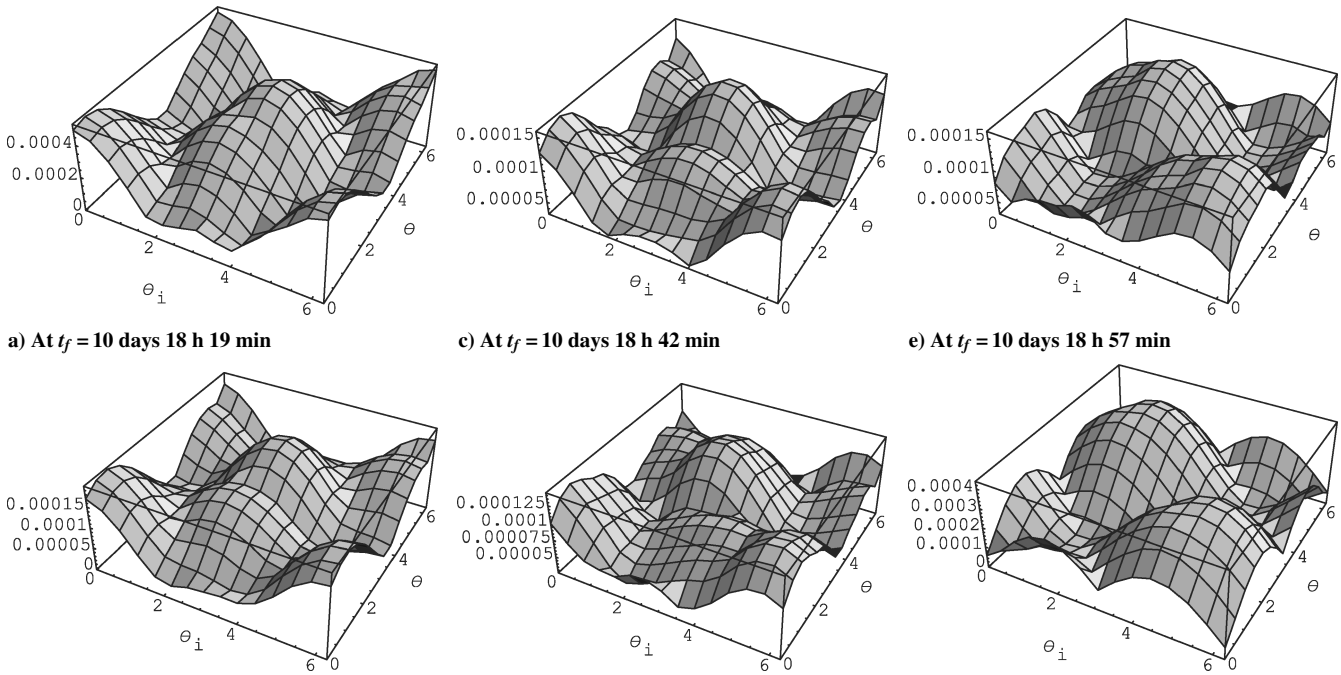

a) At $t_f = 10$ days 18 h 19 min **c) At $t_f = 10$ days 18 h 42 min** **e) At $t_f = 10$ days 18 h 57 min**

b) At $t_f = 10$ days 18 h 34 min **d) At $t_f = 10$ days 18 h 50 min** **f) At $t_f = 10$ days 19 h 13 min**

Fig. 15 Cost function as a function of the initial and final positions for several t_f.

reduced the search for stable trajectories to a boundary-value problem, we completely ignore the behavior of the spacecraft at intermediary times $t \in [0, t_f]$; we only take into account the states of the spacecraft at the initial time and at t_f. As a result, short-term oscillations play a major role and alter the locus of the minima of J. Thus, by varying t_f, we are potentially able to find infinitely many stable trajectories going through q_0 at the initial time. This aspect allows us to design a deployment problem, for instance, where several spacecraft are at the same location at the initial time and we want to place them on stable trajectories that do not collide.

Furthermore, larger or smaller values of t_f could have been chosen; however, we must be aware that if t_f is too small, short-term oscillations may be as large as the drift, and in that case, the cost function does not discriminate well. Its minima do not necessarily correspond to stable trajectories. On the other hand, if t_f is very large, the minima correspond to (M, T) stable relative trajectories with T increasing as t_f increases.

Finally, in the preceding example we selected trajectories that correspond to minima of J and let t_f vary to find several stable trajectories. However, trajectories that correspond to values of J close to the minimum may be stable trajectories as well. If we vary t_f, for example, from T^1 to T^2, we noticed that the trajectory corresponding to the minimum of J at T^1 is different from the one corresponding to the minimum of J at T^2. Although the trajectory associated to T^1 does not correspond to a minimum of J at T^2, it is stable and corresponds to a small value of J at T^2. As a result, we are able to identify regions in which there are no stable trajectories that go through an initial position q_0 and through the circle of radius r_f at t_f. For example, all stable trajectories that go through $q_0 = (495, -428.6, 247.5)$ m and $q_f = 700\cos(\theta_f)\hat{\boldsymbol{f}}_1 + 700\sin(\theta_f)\hat{\boldsymbol{f}}_2$ m at t_f are roughly localized on the arc defined by $\theta_f \in [0, \pi]$ when $t_f = 10$ days, 19 h, 13 min (Fig. 10) and by $\theta_f \in [2, 5]$ rad when $t_f = 10$ days, 18 h, 19 min (see Fig. 13 for the variation with θ_f and Fig. 14 for the trajectory at the minimum value).

D. Stable Configurations

In this section, we generalize the approach introduced earlier to design stable configurations. Without loss of generality, and for the sake of simplicity, we assume that the formation is on $\mathcal{C}_{t_0}^{r_0}$ at the initial time so that the positions of the spacecraft are determined by the angle θ_0, the angle between $\hat{\boldsymbol{f}}_1$, and the local relative position vector. As a result, the initial position may be regarded as a function of θ_0. Thus, Eqs. (21) and (22) provide a polynomial approximation of p_0 and p_f in the variables (θ_0, θ_f) (instead of θ_f only) with

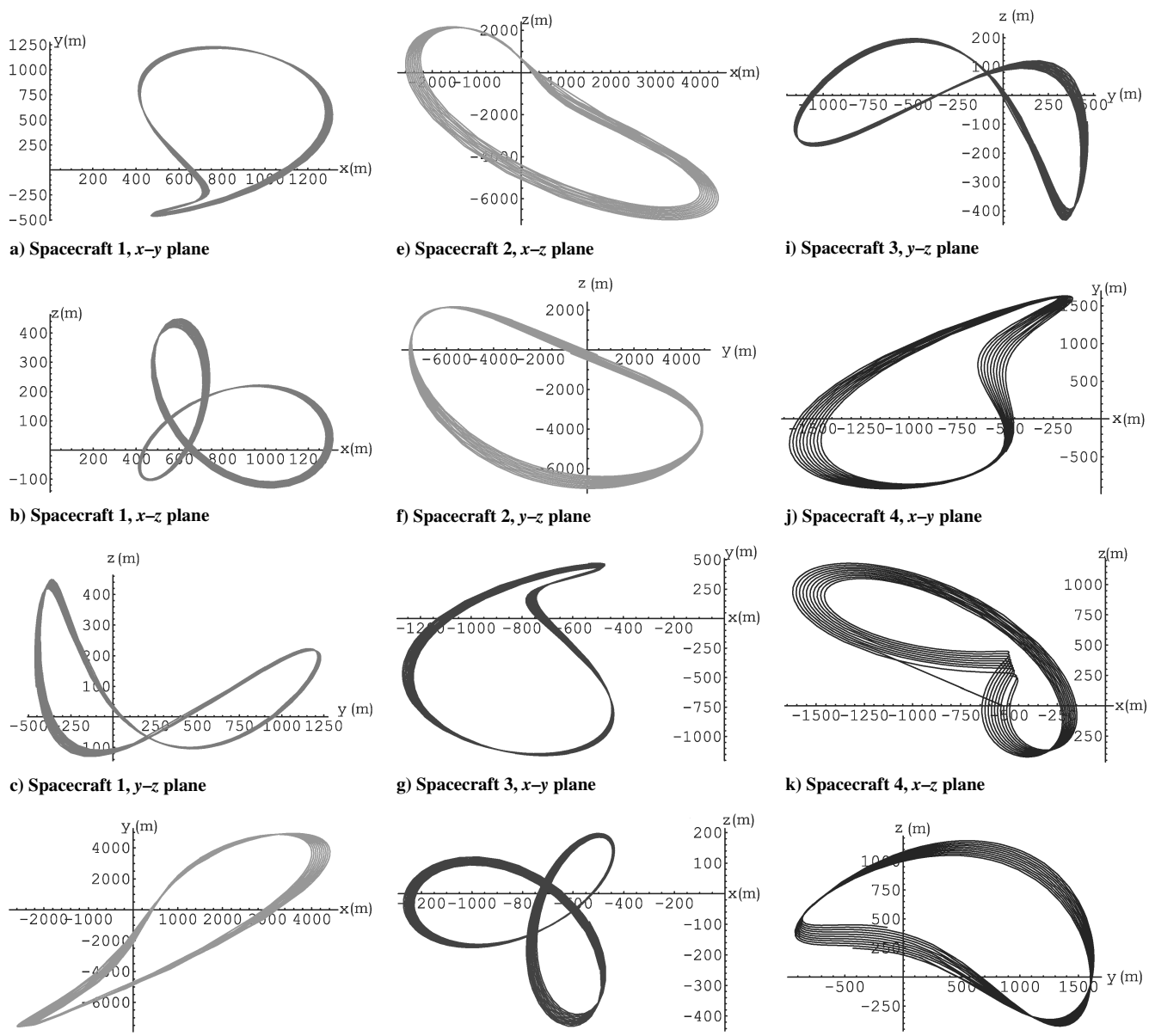

Fig. 16 Trajectories of four spacecraft found by minimizing cost function at t_f = 10 days, 18 h, 19 min.

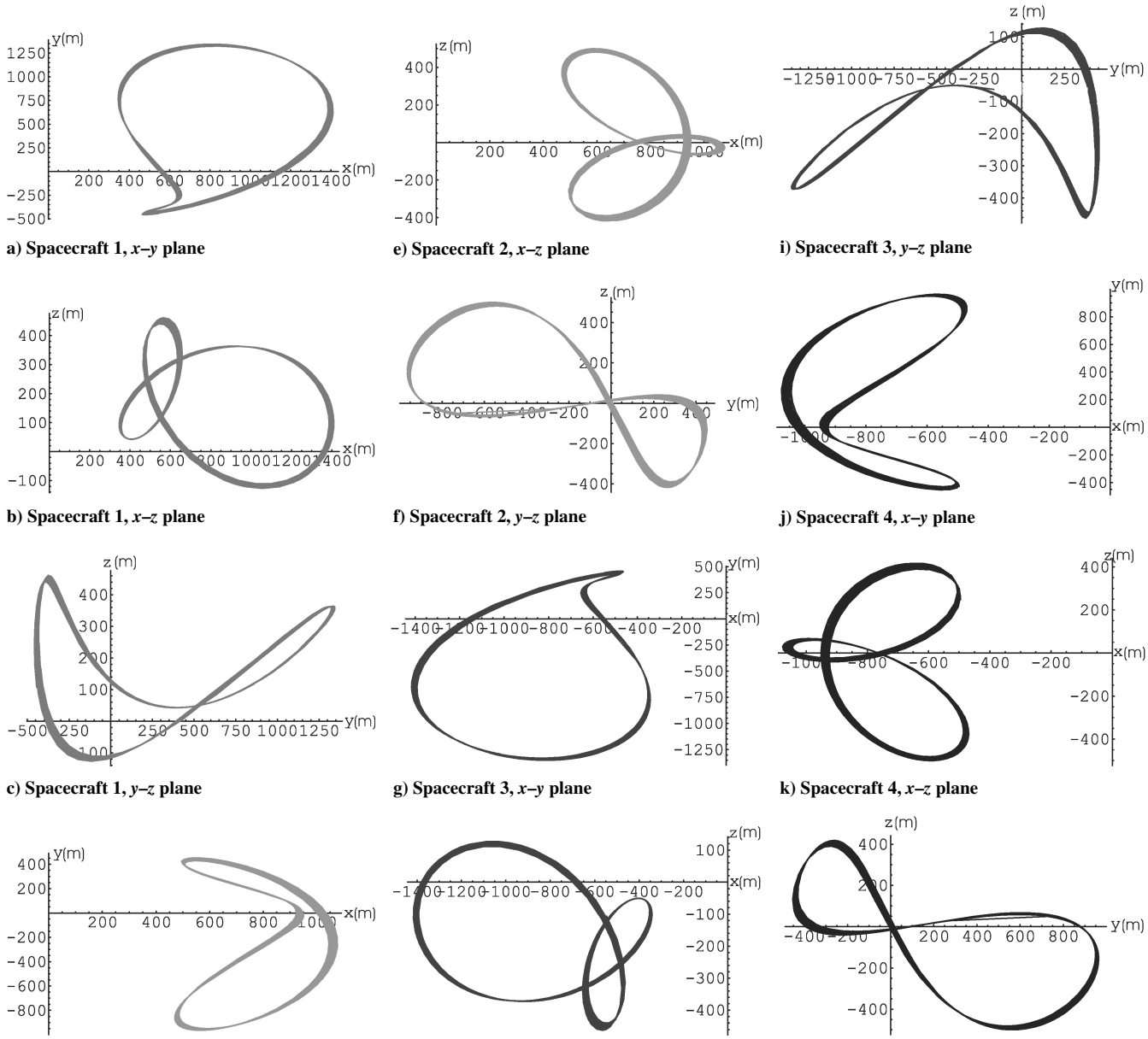

a) Spacecraft 1, *x–y* plane

b) Spacecraft 1, *x–z* plane

c) Spacecraft 1, *y–z* plane

d) Spacecraft 2, *x–y* plane

e) Spacecraft 2, *x–z* plane

f) Spacecraft 2, *y–z* plane

g) Spacecraft 3, *x–y* plane

h) Spacecraft 3, *x–z* plane

i) Spacecraft 3, *y–z* plane

j) Spacecraft 4, *x–y* plane

k) Spacecraft 4, *x–z* plane

l) Spacecraft 4, *y–z* plane

Fig. 17 Trajectories of four spacecraft found by minimizing cost function at t_f = 10 days, 19 h, 13 min.

time-dependent coefficients. The procedure to find stable trajectories is the same as before, but now we have an additional variable, θ_0. In Fig. 15, we present the values of the cost function as a function of θ_i and θ_f for different times. We notice that if two out of the three variables $(\theta_f, \theta_0, t_f)$ are given, there exists a value of the third variable that minimizes the cost function. In other words, whatever θ_0 and t_f are, there exists a stable trajectory that goes through the initial position at the initial time and reaches $\mathcal{C}_{t_f}^{r_f}$ in t_f units of time. Moreover, if t_f varies, minima of the cost function correspond to different stable trajectories due to short-term oscillations.

We consider a formation of four spacecraft equally spaced on a circle of radius 700 m about the reference trajectory that lies in the local vertical plane at the initial time. Spacecraft k has its initial position defined by $\theta_i = \pi/4 + (k-1)\pi/2$. Stable trajectories may be found by minimizing the cost function with respect to θ. For every choice of t_f, there is a solution to the minimization problem (Fig. 15). As a result, we are able to find infinitely many stable trajectories for each spacecraft. In Fig. 16, we show the trajectories of the four spacecraft that are found by considering $t_f = 10$ days, 18 h, 19 min, and in Fig. 17, $t_f = 10$ days, 19 h, 13 min. The two solutions have very different properties. Even though the positions at the final time t_f are constrained to be at 700 m from the reference trajectory in the local vertical plane, the relative distance may be large at intermediary times. For instance, the solution found for $t_f = 10$ days, 18 h, 19 min yields a formation that is as large as 6 km. Such relative distance is not accurately simulated using low-order methods. In fact, running the same computation using an order two approximation of the Hamiltonian yields a trajectory that is not as stable as the one found using the order four dynamics. The order two solution is not (6 km, t_f) stable but (15 km, t_f) stable. In addition, the order two solution does not remain (15 km, T) stable for T greater than t_f, whereas the order four solution remains (6 km, T) stable at least for $T < 1.5t_f$. (We have not checked the case $T > 1.5t_f$.) These differences in the two solutions are due to the lack of accuracy of the order two approximation over a long period of time.

V. Conclusions

We have joined elements of Hamilton–Jacobi theory and a robust algorithm that computes generating functions to address the challenges that arise in missions involving spacecraft flying in formation. Despite a complex dynamic model and an arbitrary reference

trajectory, we have been able to obtain a semi-analytic description of the phase flow as two-point boundary-value problems. Such a description of the phase space is superior in many ways to the traditional approach based on the initial-value problem. In particular, it allows us to solve two-point boundary-value problems using only simple functions evaluations. This aspect is crucial when dealing with spacecraft formations because of the combinatorial nature of the reconfiguration problem. In addition, we have shown that the algorithm we have developed is able to predict the dynamics over a long time span with high accuracy. The examples we have chosen illustrate the use of our method, but our method does not reduce to these examples and can be used to deal with more complex problems. To conclude, we recall the main feature of our method.

1) The dynamic environment may be as complex as one wants, the only constraint being that the dynamic system must be Hamiltonian. In addition, the complexity of the dynamic system does not seriously impact the computation times.

2) The reference trajectory may be arbitrary; however, it influences the domain of convergence of the series defining H^h. Techniques to estimate this domain have been developed by Guibout and Scheeres.[18]

3) The time span we consider may be very large; the larger it is, the longer the ordinary differential equations obtained with the indirect algorithm should be integrated. The main advantage of describing the phase flow as two-point boundary-value problems is that the time period we consider does not influence the accuracy of the results. This aspect is of main importance, especially as this is a weakness of traditional approaches based on the initial-value problem.

4) Our approach also allows one to deal with low-thrust spacecraft. In this case, the reconfiguration problem can be formulated as an optimal control problem whose necessary conditions for optimality are a Hamiltonian two-point boundary-value problem. For these problems, the dynamic environment may not be Hamiltonian because the necessary conditions for optimality yield a Hamiltonian system. However, it should be emphasized that the dimensionality is double (because of the adjoint variables).

5) There are no limitation on the complexity of the formation geometry in the reconfiguration problem as long as the geometry can be described with constraints on (q, p) only.

6) From the semi-analytic expression of the generating functions, several problems may be addressed. We have seen how to solve the reconfiguration problem and the deployment problem. We have also been able to find stable configurations and in previous articles the authors showed that one can also find periodic configurations. In the future, additional problems will be addressed.

Finally, the *Mathematica* package we have developed to run these simulations is freely available from the authors upon request.

Appendix: Computational Times

All of the computations have been made using *Mathematica* 5.0 on a 2-GHz processor with 2-GB RAM running under Linux.

1) Computation of the generating function F_1 up to order four over a time span of about 25 days: is about 6 h.

2) Solving the 120 two-point boundary-value problems in the first multitask missions takes about 3 min.

3) Solving the second multitask mission takes about 1 min.

4) Solving the deployment problem is instantaneous once F_1 is known.

5) Finding stable configurations is instantaneous once F_1 is known.

Acknowledgments

The work described here was funded in part by NASA's Office of Space Science and in part by the Interplanetary Network Technology Program by a grant from the Jet Propulsion Laboratory, California Institute of Technology, which is under contract with NASA.

References

[1]Hope, A. S., and Trask, A. J., "Pulsed Thrust Method for Hover Formation Flying," American Astronautical Society, AAS Paper 03-655, Aug. 2003.

[2]Vadali, S. R., Vaddi, S. S., and Alfriend, K., "An Intelligent Control Concept for Formation Flying Satellite Constellations," *International Journal of Robust and Nonlinear Control*, Vol. 12, No. 2–3, 2002, pp. 97–115.

[3]Gurfil, P., and Kasdin, N. J., "Nonlinear Modeling and Control of Spacecraft Formation Dynamics in the Configuration Space," *Journal of Guidance, Control, and Dynamics*, Vol. 27, No. 1, 2004, p. 150.

[4]Scheeres, D. J., and Hsiao, F. Y., and Vinh, N. X., "Stabilizing Motion Relative to an Unstable Orbit: Applications to Spacecraft Formation Flight," *Journal of Guidance, Control, and Dynamics*, Vol. 26, No. 1, 2003, pp. 62–73.

[5]Howell, K. C., and Marchand, B. G., "Control Strategies for Formation Flight in the Vicinity of a Libration Point Orbit," American Astronautical Society, AAS Paper 03-113, Feb. 2003.

[6]Vadali, S. R., Bae, H., and Alfriend, K. T., "Control of Libration Point Satellite Formations," American Astronautical Society, AAS Paper 04-161, Feb. 2004.

[7]Vaddi, S. S., Alfriend, K. T., and Vadali, S. R., "Sub-Optimal Formation Establishment and Reconfiguration Using Impulsive Thrust," American Astronautical Society, AAS Paper 03-590, Aug. 2003.

[8]Alfriend, K. T., and Schaub, H., "Dynamics and Control of Spacecraft Formations: Challenges and Some Solutions," American Astronautical Society, AAS Paper 00-259, March 2000.

[9]Lovell, T. A., Horneman, K. R., Tollefson, M. V., and Tragesser, S. G., "A Guidance Algorithm for Formation Reconfiguration and Maintenance Based on Perturbed Clohessy–Wiltshire Equations," American Astronautical Society, AAS Paper 03-649, Aug. 2003.

[10]Hsiao, F. Y., and Scheeres, D. J., "Design of Spacecraft Formation Orbits Relative to a Stabilized Trajectory," American Astronautical Society, AAS Paper 03-175, Feb. 2003.

[11]Hussein, I., Scheeres, D. J., and Hyland, D. C., "Control of a Satellite Formation For Imaging Applications," American Astronautical Society, AAS Paper 03-172, Feb. 2003.

[12]Mishne, D., "Maintaining Periodic Relative Trajectories of Satellite Formation by Using Power-Limited Thrusters," American Astronautical Society, AAS Paper 03-656, Aug. 2003.

[13]Alfriend, K. T., Vaddi, S. S., and Lovell, T. A., "Formation Maintenance for Low Earth Near-Circular Orbits," AAS Paper 03-652, Aug. 2003.

[14]Koon, W. S., Marsden, J. E., Masdemont, J., and Murray, R. M., "J_2 Dynamics and Formation Flight," AIAA Paper 2001-4090, Aug. 2001.

[15]Xu, Y., and Fitz-Coy, N., "Genetic Algorithm Based Sliding Method Control in the Leader/Follower Satellites Pair Maintenance," American Astronautical Society, AAS Paper 03-648, Aug. 2003.

[16]Avanzini, G., Biamonti, D., and Minisci, E. A., "Minimum-Fuel/Minimum-Time Maneuvers of Formation Flying Satellites," American Astronautical Society, AAS Paper 03-654, Aug. 2003.

[17]Wang, P. K. C., and Hadaegh, F. Y., "Minimum-Fuel Formation Reconfiguration of Multiple Free-Flying Spacecraft," *Journal of the Astronautical Sciences*, Vol. 47, No. 1–2, 1999, pp. 77–102.

[18]Guibout, V. M., "The Hamilton–Jacobi Theory for Solving Two-Point Boundary Value Problems: Theory and Numerics with Application to Spacecraft Formation Flight, Optimal Control and the Study of Phase Space Structure," Ph.D. Dissertation, Dept. of Aerospace Engineering, Univ. of Michigan, Ann Arbor, MI, Sept. 2004.

[19]Chobotov, V. A., Orbital Mechanics, 3rd ed., AIAA, Reston, VA, 2004.

[20]Guibout, V. M., and Scheeres, D. J., "Solving Relative Two-Point Boundary Value Problems: Spacecraft Formation Flight Transfers Application," *Journal of Control, Guidance, and Dynamics*, Vol. 27, No. 4, 2004, pp. 693–704.

[21]Guibout, V. M., and Scheeres, D. J., "Formation Flight with Generating Functions: Solving the Relative Boundary Value Problem," AIAA Paper 2002-4639, 2002.

[22]Guibout, V. M., and Scheeres, D. J., "Periodic Orbits from Generating Functions," American Astronautical Society, AAS Paper 2003-566, Aug. 2003.

[23]Scheeres, D. J., Park, C., and Guibout, V. M., "Solving Optimal Control Problems with Generating Functions," American Astronautical Society, AAS Paper 03-575, Aug. 2003.

[24]Greenwood, D. T., *Classical Dynamics*, Prentice–Hall, Englewood Cliffs, NJ, 1977.

[25]Goldstein, H., *Classical Mechanics*, 2nd ed., Addison–Wesley, Reading, MA, 1980.

[26]Arnold, V. I., *Mathematical Methods of Classical Mechanics*, 2nd ed., Springer-Verlag, New York, 1988.

[27]Abraham, R., and Marsden, J. E., *Foundations of Mechanics*, 2nd ed., W. A. Benjamin, Reading, MA, 1978.

[28]Guibout, V. M., and Bloch, A. M., "Discrete Variational Principles and Hamilton–Jacobi Theory for Mechanical Systems and Optimal Control Problems," *Physica D* (submitted for publication).